

# Beam test results of high $Q$ CBPM prototype for SXFEL

Jian Chen<sup>1,2</sup> · Yong-Bin Leng<sup>1</sup> · Lu-Yang Yu<sup>1</sup> · Long-Wei Lai<sup>1</sup> · Ren-Xian Yuan<sup>1</sup>

Received: 27 September 2016/Revised: 29 December 2016/Accepted: 31 December 2016/Published online: 1 March 2017  
© Shanghai Institute of Applied Physics, Chinese Academy of Sciences, Chinese Nuclear Society, Science Press China and Springer Science+Business Media Singapore 2017

**Abstract** In pursuit of high-precision beam position measurements at micrometers or submicrometers for the Shanghai soft X-ray free-electron laser (SXFEL) facility which is under construction in the vicinity of the Shanghai Synchrotron Radiation Facility, a high  $Q$  cavity beam position monitor (CBPM) with a resonant frequency of 4.7 GHz is developed by the Shanghai Institute of Applied Physics, and the relevant BPM electronics with a dedicated RF front end, and a digital BPM, are completed. The cavity design, cold test, system architecture, and first beam test are performed at the Shanghai deep ultraviolet free-electron laser (Zhao et al. in Nucl Instrum Meth A 528(1–2): 591–594, 2004. doi:10.1016/j.nima.2004.04.108) facility. Results of the beam experiment show that the performance of the CBPM is consistent with basic expectations, and the beam position resolution can fulfill the requirements for the SXFEL project if the beam conditions are optimized.

**Keywords** High  $Q$  CBPM · SXFEL · Position resolution · RF front end · DBPM

## 1 Introduction

The Shanghai soft X-ray free-electron laser (SXFEL) is an official XFEL facility. It will provide a fully coherent light source and serve to verify key FEL schemes and technologies covering two-stage cascaded high-gain harmonic generation (HGHG), with an expected capacity to generate 9-nm X-ray laser by adopting an FEL frequency doubling of ultraviolet band seeded laser of 265 nm [2]. The SXFEL facility, constructed on the basis of the HGHG or EEHG scheme, has a strict beam position resolution requirement, being 1  $\mu\text{m}$  at 0.5 nC, to ensure that the electron beam overlaps the generated photon beam stringently and that both can pass through the entire undulator section. Among the various types of BPMs, the cavity BPM can adopt to a resonant cavity structure and through the use of antisymmetric characteristic modes, coupled from the cavity, to measure beam position and can reach a submicrometer even nanometer level position resolution has become a critical beam instrumentation component for FEL [3, 4].

For a CBPM, the quality factor ( $Q$ ) is an important parameter. A cavity of low  $Q$  factor means high efficiency of the coupling structure, featuring broad band width, short-duration time, and higher temporal resolution, whereas a high  $Q$  cavity coupling structure is of low efficiency, narrow bandwidth, long-duration time, and lower temporal resolution. So, the  $Q$  value selection needs to match with the whole CBPM system and meets the working mechanism of the FEL facility.

In European X-ray FEL (EXFEL), a low  $Q$  CBPM for a multibunch working mechanism with a resonant frequency of 3.3 GHz was developed and combined with relevant electronics, achieving position resolutions of well below

---

This work was supported by the National Natural Science Foundation of China (Nos. 11575282 and 11305253).

---

✉ Yong-Bin Leng  
lengyongbin@sinap.ac.cn

<sup>1</sup> Shanghai Institute of Applied Physics, Chinese Academy of Sciences, Shanghai 201204, China

<sup>2</sup> University of the Chinese Academy of Sciences, Beijing 100049, China

1- $\mu\text{m}$  rms [5, 6]. For the Swiss FEL, two types of cavity BPM are used. The low  $Q$  CBPM used in the Linac can easily separate two adjacent bunches of a 28-ns bunch spacing, while BPM pickups of the same basic structure, but with higher  $Q$  value, are used in the undulators that receive only single bunches and have higher resolution and precision requirements [7]. SPring-8 designed a low  $Q$  cavity BPM with a resonant frequency of 4.76 GHz, with the position resolution of  $<0.2\ \mu\text{m}$  at a 0.3-nC bunch charge [8, 9]. KEK designed a low  $Q$  interaction point BPM (IP-BPM) and achieved a beam position resolution at a normalized charge (1.6 nC) with three low  $Q$  IP-BPMs at 22 nm [10]. In SLAC, a new X-band CBPM with a high  $Q$  factor was developed for the LCLS-II, and combining with an improved receiver and digitizer, they will provide a single-shot position resolution of 50 nm, rather than 200 nm of the LCLS at bunch charge of 200 pC (no experiment results yet) [11, 12]. In China, Hefei light source (HLS) designed a S-band re-entrant cavity BPM with a high  $Q$  factor, and the cold test results showed a position resolution better than 3  $\mu\text{m}$  (no beam test results yet) [13].

A low  $Q$  cavity was designed and tested by our group [14–16]. It features many of the strengths, but the performance was limited by the electronics due to the short-duration time. Considering the single-bunch working mechanism of SXFEL, and for matching the electronics to increase the processing gain to achieve a higher resolution, we redesigned and chose a high  $Q$  CBPM as the beam position measurement scheme. In addition, relevant electronic components were developed and, as a preliminary performance test, an array of three adjacent high  $Q$  cavity BPMs was installed at the SDUV-FEL facility.

## 2 Measurement principle of CBPM

For a cylindrical pill-box cavity, when the beam source runs along the  $z$ -axis, the bunch does not lose energy in the transverse electric field of the TE mode. However, because of the longitudinal electric field of the TM mode, the bunch loses energy in the longitudinal electric field excited by itself and effectively induces the excitation mode. Therefore, only the TM modes are excited and the amplitude is determined by the bunch energy that is lost. The axial electric field component of the TM<sub>110</sub> mode in cylindrical coordinates can be expressed by Eq. (1):

$$E_z(\rho, \phi, z) = E_0 J_1\left(\frac{\chi_{11}\rho}{r}\right) \cos \phi, \quad (1)$$

where  $E_0$  is the amplitude of the electric field and  $J_1$  is the first-order Bessel function of the first kind,  $\chi_{11}$  is the first root of  $J_1(\rho) = 0$ ,  $r$  is the cavity radius,  $\phi$  is the angle

between the field of TM<sub>110</sub> mode and axial direction, and  $\rho$  is the radial coordinate.  $J_1(\rho)$  is proportional to  $\rho$  when  $\rho \sim 0$ . Thus, the excited voltage of the TM<sub>110</sub> mode is proportional to the beam offset  $x$  and beam charge  $q$ :

$$V_z = A_0 q x. \quad (2)$$

In order to eliminate the beam charge variation effect, an additional monopole mode cavity shall be employed, and the signal amplitude of the monopole mode is independent to the beam position but proportional to the beam charge only.

Due to limited quality factor of the cavity, the energy of all the electromagnetic field modes excited by the cavity has three tracks. Some is stored inside the cavity, a small portion is lost on the metal wall, and some is coupled out by the appropriate coupling structure, which can be detected by the following electronics.

However, when a bunch of particle beam transits the cavity close to the  $z$ -axis, the TM<sub>010</sub> mode obtains much of the lost energy; thus, the amplitude is larger than that of the TM<sub>110</sub> mode, with a certain amount of crossover in the bandwidth. Therefore, it is important to design an appropriate coupling structure, which outputs the TM<sub>110</sub> mode effectively and damps most of the power from the TM<sub>010</sub> mode in the meantime. It affects greatly the measurement of position resolution, too [17].

## 3 Cavity pickup

On the basis of the defects of low  $Q$  cavity by beam test, we redesigned a high  $Q$  cavity BPM to strategically address the above considerations. The pre-designed parameters of the high  $Q$  CBPM are given in Table 1. The working frequency of 4.70 GHz was chosen due to considering the vacuum pipe radius of 8 mm and avoiding dark current from the accelerating system. Cavity material was changed from stainless steel 304 to oxygen-free copper, which raises theoretically the  $Q$  value to 7786 and 3120 for the position and reference cavities, respectively.

**Table 1** Pre-designed parameters of the high  $Q$  CBPM

Cavity parameter	Position cavity	Reference cavity
Resonant frequency	4.70 GHz	4.70 GHz
Loaded $Q$ factor	7786	3120
Unloaded $Q$ factor	8244	3305
External $Q$ factor	$1.401 \times 10^5$	$5.573 \times 10^4$
Normalized shunt impedance $[R/Q]$	$2.02\ \Omega/\text{mm}^2$	81.38 $\Omega$
Number of ports	4(X:2, Y:2)	2

The three-dimensional structure of the cavity, which consists of seven parts, is shown in Fig. 1. The total length of the probe is kept at 112 mm, but the distance between the two cavities increased from 35 to 45 mm so as to reduce the possibility of signal coupling between them. The reference cavity has more ports to facilitate cold testing, and the coupling structure changes from magnetic coupling to weaker electric coupling.

Considering the complexity of setting up a platform to test the cavity, we developed a convenient and effective method to test the resonant frequency and the  $Q$  factor of cavity by using the Agilent (Santa Clara, CA, USA) N5230A PNA-L network analyzer. We measured S21 parameters, designated the frequency of peak as the cavity working frequency, and obtained the  $Q$  factor by measuring the 3 dB bandwidth. As shown in Fig. 2, the cold test results of the cavity is 4.678 and 4.686 GHz for the position cavity and 4.695 GHz for the reference cavity, which accord well with the designed value of 4.70 GHz. However, the correspondent  $Q$  factor differs greatly from the design.

### 4 System setup

In order to check whether the actual performance can achieve the theoretical design we expected, and to test the whole BPM system we developed, the beam test was conducted on the SDUV facility. The BPM system consists of a cavity BPM, a dedicated RF front end, and a home-made digital BPM processor.

Figure 3 shows an array of three BPM pickups installed at the SDUV test injector facility. The middle cavity (CBPM2) was mounted on a movable stage to imitate the beam offset.

Because of limitations of ultrahigh-speed ADC resolution, precise measurements at submicrometer level are difficult to achieve with RF sampling methods. It is essential to adopt RF receiver architecture that converts the RF signal to intermediate frequency (IF) to be digitized by

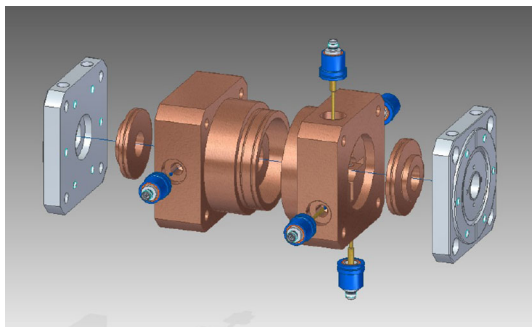


Fig. 1 Three-dimensional structure of the high  $Q$  CBPM

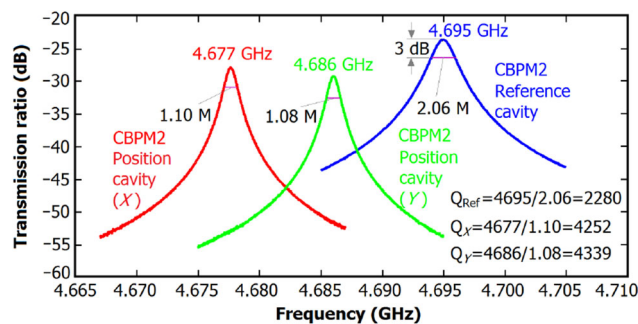


Fig. 2 Cold test results of the cavity

high-resolution ADC. The RF front end is shown schematically in Fig. 4 [18].

An input band-pass filter (BPF) selects the cavity signal components at 4.7 GHz to suppress other harmonics coupling from the cavity or the spatial disturbance into the low-noise amplifier (LNA) that follows. The LNA with 45-dB gain is used to adjust the signal intensity from the BPF and to acquire a broader dynamic range. The down-conversion operates with an LO and converts the RF signal to IF, which ranges from DC to hundreds of megahertz. Generally, we convert the RF signal to IF at 500 MHz, depending on performance of the DBPM. An adjustable IF amplifier accomplishes the last gain adjustment to fulfill the input requirement of ADCs and with a BPF having a center frequency of 500 MHz and bandwidth of 10 MHz as an antialiasing filter to suppress other amplified harmonics. Both of them are integrated into the DBPM.

The DBPM was developed by our group several years ago (Fig. 5) [19–21]. Based on software radio architecture, it adopts band-pass sampling technology as the quantization scheme, which consists of a RF pre-processing module, an ADC module, and a digital board module. It has been in good performances. The basic parameters are sampling rate, 117 MHz; center frequency, 500 MHz; band width, 10 MHz; ADC resolution, 16 bit; ENOB, >10 bit; and dynamic gain range, 60 dB.

### 5 Beam test

The beam test was performed on the basis of the cold test. A broadband oscilloscope was used to evaluate the CBPM performance directly; the calibration factor and position resolution were also measured by the entire BPM system.

#### 5.1 Cavity evaluation

The signal data collected by the broadband oscilloscope were processed using MATLAB. The CBPM output signal

**Fig. 3** The BPM test array installed at the SDUV test injector facility and the arrangement

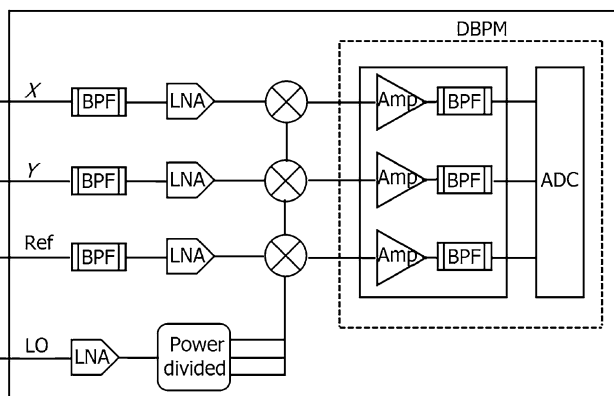
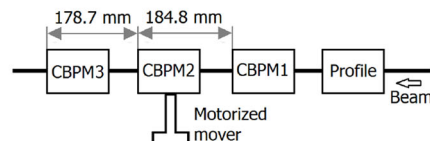
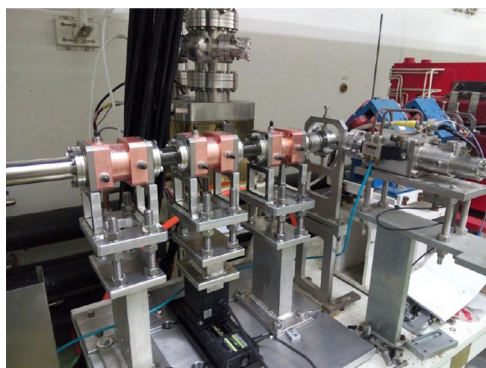


**Fig. 4** Schematic of the RF front end

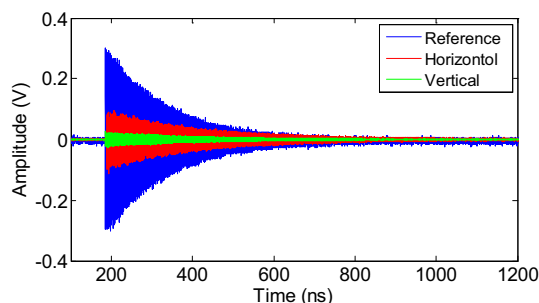


**Fig. 6** RF signals waveform of CBPM

frequency of three CBPM position cavities has a good consistency, but they differ greatly from the reference cavity frequency, which is caused by solder melts into the reference cavity in welding.

As shown in Fig. 8,  $Q$  values of the reference and position cavities are 2134 and 4261, respectively, which is in accordance with the cold test. The cavity decay time can be calculated in the frequency domain and fit into the time domain. In the frequency domain, the decay time can be calculated by Eq. (3):

$$\tau = Q / (2\pi f_L), \tag{3}$$

where  $f_L$  is the resonant frequency. Thus, the decay time values of the reference and position cavities are calculated at 73 and 145 ns, respectively.

In the time domain, the data-fitting method can help to obtain the decay time directly. However, some pre-treatment is necessary for the original data, such as a digital filter to remove the influence of harmonics. Figure 9 shows the result of 77 ns for reference cavity (144 ns for the position cavity) processed in the time domain, which is close to the result processed in the frequency domain.

The results of cavity evaluation generally agree with the design except for the quality factor. The measured  $Q$  factors are significantly smaller than the design value. As the cavity was made by brazing two assembly parts and the faying face had some distance from the locating

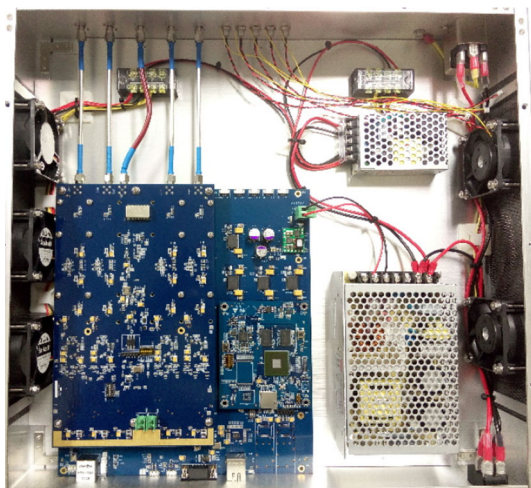


**Fig. 5** The DBPM

waveform is shown in Fig. 6. The CBPM spectra of the reference and position cavities are shown in Fig. 7.

According to the figures mentioned above, the RF signal waveform in the time domain is consistent with the theoretical expectations. The signal spectra of the reference and position cavities are well in accordance with those of the cold test. We also find that the resonant

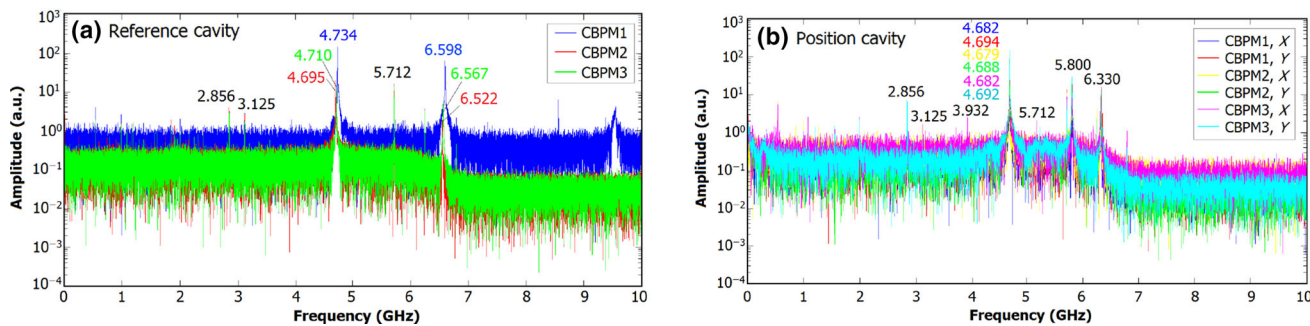


Fig. 7 CBPM spectra of the reference (a) and position (b) cavities

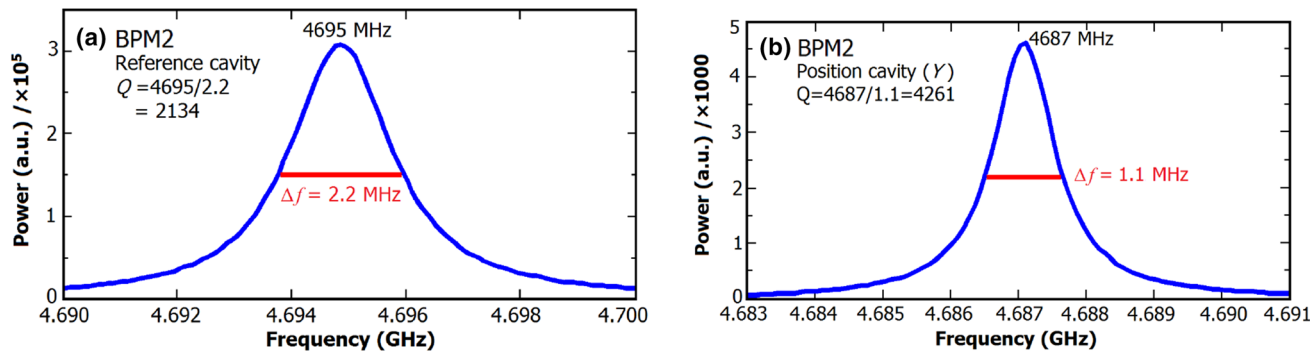


Fig. 8  $Q$  values of the reference (a) and position (b) cavities.  $\Delta \times 10^5$

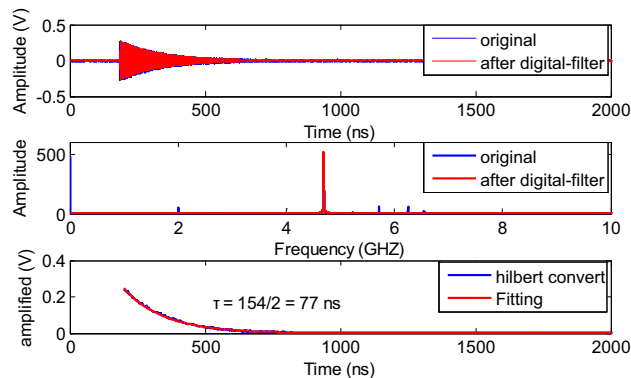


Fig. 9 Decay time of the reference cavity processed in the time domain

face, the welding seam could cause the energy loss more seriously. This is the most probable factor for the unloaded  $Q$  factor being smaller than expected. However, it also can meet the requirements for the project based on the BPM system.

### 5.2 IF pulse shape

The RF signal output from the cavity is directed down converted to a low intermediate frequency by this RF front end and is sampled by a signal processor. Two LO were

used to obtain the IF signals about 30 and 500 MHz to verify the RF front end, respectively. Figure 10 shows the IF waveforms sampled by broadband oscilloscope with an LO of 4665 MHz. A LPF of DC to 32 MHz was also used to suppress the high-frequency component generated by the mixer. The waveform and spectrum are in accordance with the theory.

With the RF front end and DBPM, IF signals at 500 MHz were sampled. Because of the sub-Nyquist sampling method, the frequency of the IF signals was transferred to the first Nyquist zone. The waveforms and spectra are shown in Fig. 11. The IF signal waveforms and corresponding spectra are in line with expectations that prove the RF front end can be applied in the high  $Q$  CBPM system.

### 5.3 Calibration

The calibration factor is required to convert the position of beam offset. A two-dimensional motion platform was installed under one of the cavities which can imitate the beam offset from  $-2$  to  $2$  mm, with a step of  $200 \mu\text{m}$ , in both the horizontal and vertical directions. The calibration system is shown schematically in Fig. 12a. The data were collected by the DBPM and processed in the frequency domain with MATLAB. Figure 12b shows the calibration factor of the CBPM in vertical direction.

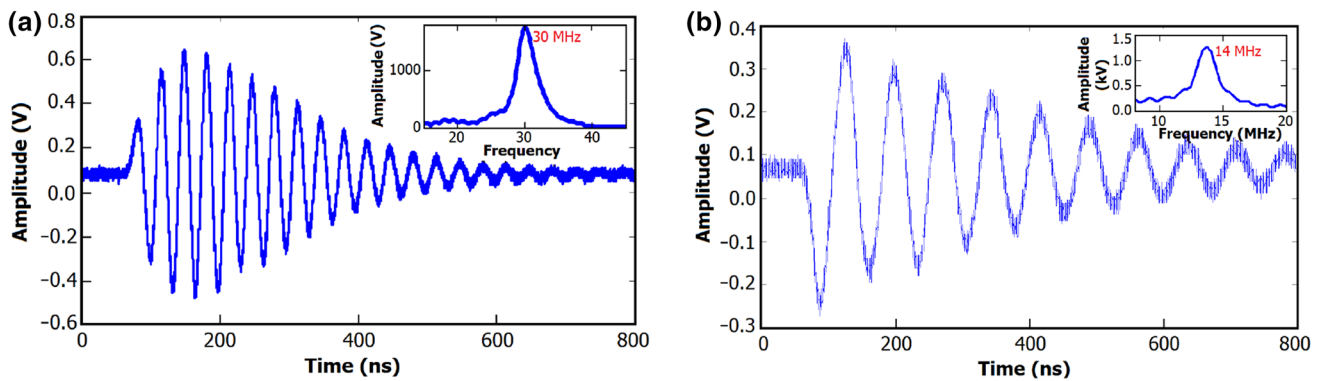


Fig. 10 IF waveforms of reference cavity (a) and vertical position cavity (b) sampled by broadband oscilloscope

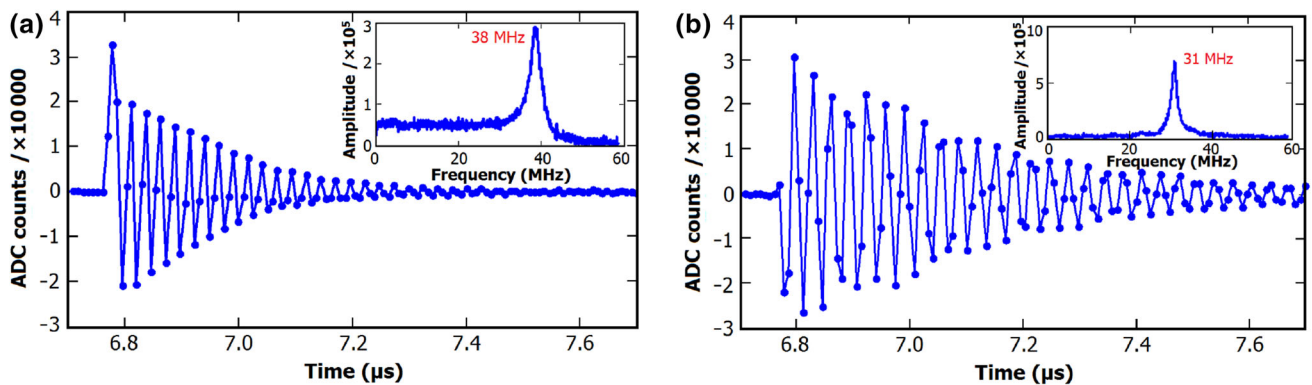


Fig. 11 IF waveforms of reference cavity (a) and horizontal position cavity (b) sampled by DBPM

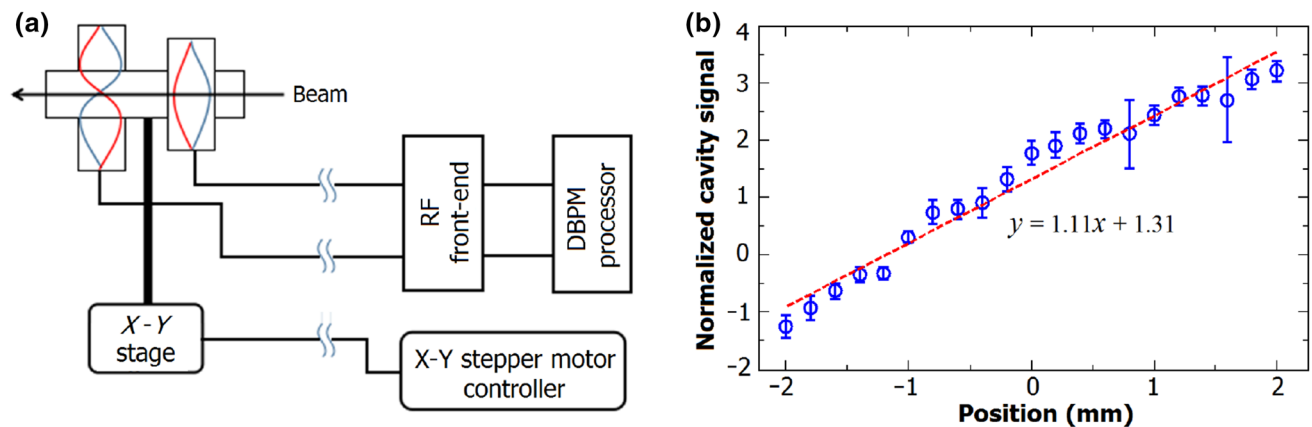


Fig. 12 The calibration system (a) and the calibration factor of the CBPM in vertical direction (b)

### 5.4 Position resolution

The position resolution was measured on the basis of correlating readings of the three cavities, as shown in Fig. 13.

By using the geometric relationships in Eq. (4), the position reading of CBPM2 ( $U_2'$ ) can be estimated by the position reading of CBPM1 and CBPM3 ( $U_1$  and  $U_3$ ). Also, a position reading of CBPM2 could be obtained by

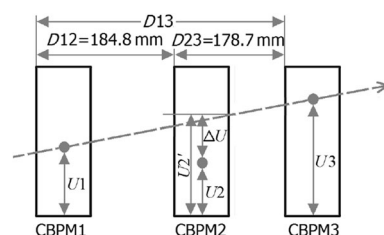


Fig. 13 Schematic of the position resolution measurement

itself ( $U2$ ). To calculate the difference between  $U2$  and  $U2'$  ( $\Delta U$ ) with the assumption that all BPMs have equal position jitters, the position resolution can be calculated by Eq. (5), where GF is a geometric factor related to the location of the three cavities and can be calculated by Eq. (6),  $\text{std}_{\Delta d}$  is the standard deviation of  $\Delta d$ , and  $\Delta d$  is the difference in position converted by the calibration factor and  $\Delta U$ .

$$U2' = (D12 \cdot U3 + D23 \cdot U1)/D13, \tag{4}$$

$$\delta_{\text{CBPM}} = \text{GF} \cdot \text{std}_{\Delta d}, \tag{5}$$

$$\text{GF} = \frac{1}{\sqrt{\left(\frac{D23}{D13}\right)^2 + \left(\frac{D12}{D13}\right)^2 + 1}}. \tag{6}$$

In the experiment, 1000 sets of data were sampled by the DBPM and were processed offline, with the bunch charge of 20 pC. The gain setting of the RF front end was chosen to provide a linear measurement range of  $-2$  to  $2$  mm. By using the reference cavity signals to normalize the position cavity signals and with the position of beam offset converted by calibration factor, the position measured and the expected values of the CBPM2 could be obtained (Fig. 14).

The  $\Delta d$  distributions were calculated (Fig. 15), and the CBPM system's position resolution in vertical direction is  $23 \mu\text{m}$ .

Because the SDUV facility is a test bed only, most of the time it works at a low-charge state (20–30 pC). The beam jitter is also somewhat significant, so we set the linear measurement range at  $\pm 2$  mm. However, for the SXFEL facility, the charge will be set at 0.5 nC and the beam jitter will be kept within  $\pm 500 \mu\text{m}$ .

In theory, increasing the bunch charge from 0.5 to 20 pC means a gain of  $25\times$ . Meanwhile, with the measurement range maintained within  $\pm 500 \mu\text{m}$ , we can achieve an electronics gain by  $4\times$ . Considering that the most ideal conditions and the noise of the whole system have not changed a great deal, we can achieve a position resolution

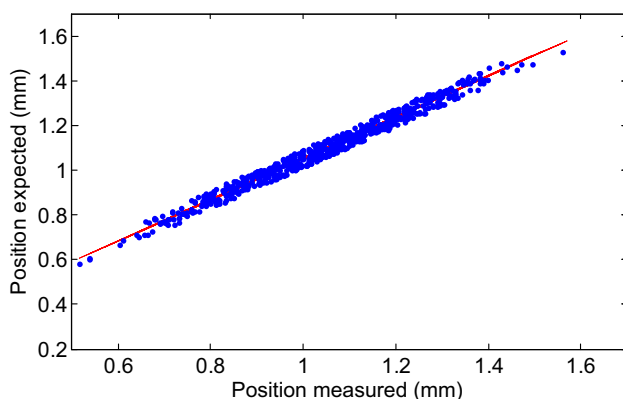


Fig. 14 Relationship of the position measured and expected

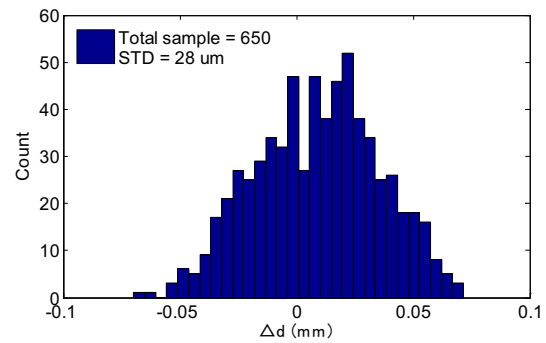


Fig. 15 Histogram of the  $\Delta d$  with 650 samples

of  $0.23 \mu\text{m}$ . Related experiments will be conducted in subsequent research.

## 6 Conclusion

We have completed the entire CBPM system and conducted the first test in the SDUV facility. The aim is to evaluate the performance of the newly designed high  $Q$  CBPM and of the whole CBPM system in preparation for the construction of the SXFEL. The results show that the cavity performance meets the needs of the project, although the quality factor was less than the design value. We obtained a position resolution of  $23 \mu\text{m}$  when the bunch charge was 20 pC, and the linear measurement range was  $\pm 2$  mm. By theoretical calculations, we can easily fulfill the resolution requirement of  $1 \mu\text{m}$  at 0.5 nC for the SXFEL if we raise the bunch charge and control the measurement range.

## References

1. Z.T. Zhao, Z.M. Dai, X.F. Zhao et al., The Shanghai high-gain harmonic generation DUV free-electron laser. *Nucl. Instrum. Meth. A* **528**(1–2), 591–594 (2004). doi:10.1016/j.nima.2004.04.108
2. Shanghai Soft X-ray FEL (SXFEL), Conceptual design report (2015)
3. T. Slaton, G. Mazaheri et al., TH4064: development of nanometer resolution C-band radio frequency beam position monitors in the final focus test beam. in *Proceeding of LINAC*, Chicago, USA, 23–28 August 1998
4. S. Walston, S. Boogert et al., Performance of a high resolution cavity beam position monitor system. *Nucl. Instrum. Meth. A* **578**(1), 1–22 (2007). doi:10.1016/j.nima.2007.04.162
5. M. Stadler, R. Baldinger, R. Ditter et al., TUPA27: beam test results of undulator cavity BPM electronics for the European XFEL. in *Proceeding of IBIC*, Tsukuba, Japan, 1–4 October 2012
6. M. Stadler, R. Baldinger, R. Ditter et al., WEPD12: Low- $Q$  cavity BPM electronics for E-XFEL, Flash-II and SwissFEL. in *Proceeding of IBIC*, Monterey, CA, USA, 14–18 September 2014

7. M. Stadler, R. Baldinger, R. Ditter et al., WEPD13: development of the SwissFEL undulator BPM system. in *Proceeding of IBIC*, Monterey, CA, USA, 14–18 September 2014
8. H. Maesaka, S. Inoue, T. Ohshima et al., MOPD07: development of the RF cavity BPM of XFEL/SPRING-8. in *Proceeding of DIPAC*, Basel, Switzerland, 25–27 May 2009
9. H. Maesaka, H. Ego, S. Inoue et al., Sub-micron resolution rf cavity beam position monitor system at the SACLA XFEL facility. *Nucl. Instrum. Meth. A* **696**, 66–74 (2012). doi:[10.1016/j.nima.2012.08.088](https://doi.org/10.1016/j.nima.2012.08.088)
10. S. Jang, E-S. Kim, J.G. Hwang et al., THPME147: the high position resolution cavity BPM developments and measurement for ILC final focus system. in *Proceeding of IPAC, Dresden*, Germany, 15–20 June 2014
11. A. Young, J. Frisch, S. Smith et al., MOPG019: new low cost X-Band cavity BPM receiver. in *Proceeding of BIW*, Newport News, VA USA, 15–19 April 2012
12. S. Smith, S. Hoobler, R.G. Johnson et al., TUOC03: LCLS cavity beam position monitors. in *Proceeding of DIPAC*, Basel, Switzerland, 25–27 May 2009
13. Q. Luo, B.G. Sun, Q.K. Jia et al., Design and cold test of S-band cavity BPM for HLS. *Sci. China Phys. Mech. Astron.* **54**(2), 292–295 (2011). doi:[10.1007/s11433-011-4555-y](https://doi.org/10.1007/s11433-011-4555-y)
14. R.X. Yuan, W.M. Zhou, Z.C. Chen et al., Design and test of SX-FEL cavity BPM. *Chin. Phys. C* **37**(11), 118001 (2013). doi:[10.1088/1674-1137/37/11/118001](https://doi.org/10.1088/1674-1137/37/11/118001)
15. B.P. Wang, Y.B. Leng, L.Y. Yu et al., Design and measurement of signal processing system for cavity beam position monitor. *Nucl. Sci. Tech.* **24**(2), 020101 (2013). doi:[10.13538/j.1001-8042/nst.2013.02.007](https://doi.org/10.13538/j.1001-8042/nst.2013.02.007)
16. J. Chen, Y.B. Leng, L.Y. Yu et al., MONP049: beam experiment of low Q CBPM prototype for SXFEL. in *Proceeding of IPAC*, Busan, Korea, 8–13 May 2016
17. J.H. Chu, *Development of C Band Cavity Beam Position Monitor and RF Front End Signal Processing System*. (Ph.D. Thesis, Shanghai Institute of Applied Physics, CAS, 2008)
18. P. Eskelinen, *Introduction to RF Equipment and System Design* (Artch House Inc. Wiley-Interscience, Hoboken, 2004)
19. Y. Xing, *Research of Signal Conditioning and High Speed Data Acquisition Techniques for Particle Acceleration Beam Diagnostics*. (Ph.D. Thesis, Shanghai Institute of Applied Physics, CAS, 2012)
20. X.D. Sun, Y.B. Leng, Implementation and integration of a systematic DBPM calibration with PLL frequency synthesis and FPGA. *Nucl. Sci. Tech.* **25**(2), 020401 (2014). doi:[10.13538/j.1001-8042/nst.25.020401](https://doi.org/10.13538/j.1001-8042/nst.25.020401)
21. L.W. Lai, Y.B. Leng, X. Yi et al., DBPM signal processing with field programmable gate arrays. *Nucl. Sci. Tech.* **22**(3), 129–133 (2011). doi:[10.13538/j.1001-8042/nst.22.129-133](https://doi.org/10.13538/j.1001-8042/nst.22.129-133)